



Universidad Autónoma de Querétaro

Facultad de Ingeniería

Licenciatura en Ingeniería Física

Monte Carlo Simulations of Self-Assembly of Soft Spheres Confined in Cylindrical Geometries

TESIS

Que como parte de los requisitos para obtener el grado de
Licenciado en Ingeniería Física

Presenta:

Juan Germán Caltzontzin Rabell

Dirigido por:

Dr. Saúl Iván Hernández Hernández

SINODALES

Dr. Saúl Iván Hernández Hernández

Presidente

Firma

Dr. Adolfo Huet Soto

Secretario

ADOLFO HUET SOTO

Firma

Dr. Aldrin Melitón Cervantes Contreras

Sinodal

Firma

Dra. María Lucero Gómez Herrera

Vocal

Firma

Dr. Manuel Toledano Ayala
Director de la facultad

Centro Universitario
Querétaro, QRO
México.
junio 2019

© 2019 - Juan Germán Caltzontzin Rabell

GNU General Public License

A todos los que han contribuido a hacerme quien soy

Acknowledgments

Agradezco a mis padres, a mis hermanos, a mi abuela y a mi familia en general por su apoyo constante e incansable. También agradezco especialmente a mis maestros y a mis compañeros y amigos de la licenciatura. En general agradezco a todos aquellos que me han soportado en algún momento de sus vidas y a todos los que me han enseñado o compartido algo.

Investigación realizada gracias al Programa de Apoyo a Proyectos de Investigación e Innovación Tecnológica (PAPIIT) de la UNAM IA104319 y al proyecto LANCAD-UNAM-DGTIC-276.

Abstract

By using Monte Carlo simulations of core-corona colloidal particles, we explore the low-temperature equilibrium morphologies that arise from the interplay between the breaking of translational symmetry (due to two-dimensional confinement), and the tendency of these materials to self-assemble into complex lattices. We found several structures as the density, confinement size and interaction range are varied. The morphological characterization of the different particle configurations is performed with a procedure based on a projection of the 3D particle positions over a two-dimensional flat surface.

Resumen

Implementando simulaciones de Monte Carlo para un sistema coloidal de esferas suaves, se exploran las morfologías de equilibrio a bajas temperaturas que surgen de la interacción entre el rompimiento de la simetría traslacional debido al confinamiento y la tendencia de estos materiales a autoensamblarse en redes complejas. Se encuentran varias estructuras al variar la densidad, el tamaño del confinamiento y la distancia de interacción. La caracterización morfológica es llevada a cabo basada en una proyección del sistema 3D a una superficie plana.

Contents

Acknowledgments	vii
Abstract	ix
Resumen	xi
Contents	xiii
List of Figures	xv
1 Introduction	1
1.1 Motivation	1
1.2 Problem Formulation	2
1.3 Objectives	2
1.3.1 Specific Objectives	2
1.4 Thesis Structure	3
2 Literature Survey	5
2.1 Background	5
2.2 Colloids	5
2.3 Block copolymers	5
2.4 Two-dimensional Bravais Lattices	5
2.5 Coordination number	6
2.6 Sphere packaging	6
2.7 Statistical Physics	7
2.7.1 Statistical ensembles	7
2.7.2 Partition function	7
2.8 Reduced units	8
3 Methodology	9
3.1 Model: Core-corona potential	9
3.2 Phase-characterization procedure	10
3.2.1 Hexatic order parameter	10
3.2.2 Mean coordination number	10
3.3 Packaging Factor	10

3.4	Design	10
3.4.1	Monte Carlo simulations specifications	10
3.5	Implementation	11
4	Results and Discussion	13
4.1	Results	13
4.1.1	Hexatic order parameter	15
4.1.2	Packaging factor	17
4.1.3	Coordination number	20
4.2	Discussion	24
4.3	Significance/Impact	25
4.4	Future Work	25
5	Conclusion	27
	References	31
.1	Codes	32

List of Figures

1.1	Some tantalizing natural patterns	2
3.1	Model	9
4.1	Equilibrium configuration for the parameters $\lambda = 2, r = 3.5, \rho = 0.6$	13
4.2	Equilibrium configuration for the parameters $\lambda = 2.5, r = 3.5, \rho = 1$	14
4.3	Projection of the two biggest layers for the parameters $\lambda = 2.0, r = 4.0, \rho = 0.6$. . .	14
4.4	hexatic order parameter of the second biggest layer	15
4.5	hexatic order parameter of the second biggest layer	15
4.6	hexatic order parameter of the second biggest layer	16
4.7	hexatic order parameter of the biggest layer	16
4.8	hexatic order parameter of the biggest layer	17
4.9	hexatic order parameter of the biggest layer	17
4.10	packaging factor of the second biggest layer	18
4.11	packaging factor of the second biggest layer	18
4.12	packaging factor of the second biggest layer	19
4.13	packaging factor of the biggest layer	19
4.14	packaging factor of the biggest layer	20
4.15	packaging factor of the biggest layer	20
4.16	average coordination number of the second biggest layer	21
4.17	average coordination number of the second biggest layer	21
4.18	average coordination number of the second biggest layer	22
4.19	average coordination number of the biggest layer	22
4.20	average coordination number of the biggest layer	23
4.21	average coordination number of the biggest layer	23
4.22	An unexpected configuration. $\lambda = 4, \rho = 0.2, r = 3.5$	24

Introduction

In a confined many-particle system, the equilibrium configuration is determined by the interactions between particles, and the effect of the boundaries. The mathematical problem of finding the lowest-energy configuration of a given system is of great interest and has been studied for hard spheres confined into a cylinder[1]. As the structure of a material plays a significant role in the determination of its properties, this problem is particularly important in materials science. There are two approaches to create a material with a designed morphology: top-down and bottom-up. The latter has been the subject of great development in recent years[2]. It consists in the self-assembly of small units to form larger structures. Computational simulations of such systems provide great insights on the governing parameters given place to specific particle arrangements.

Systems polymer-grafted colloidal particles can be represented by a core-corona potential; which has two repulsive length scales, one associated to the impenetrable hard core and the other one, associated to the soft repulsive corona. The ratio between these two repulsive interaction lengths, λ , can be used as a control parameter to generate a great variety of morphologies, like striped phases. These particular type of systems have received a lot of attention due possible technological applications that includes nanolithography and photonic crystals.

Previous research on two-dimensional systems has shown that the emergence of striped phases can also be associated to the interplay of purely repulsive interaction lengths, and no only as the competition between short-ranged attractive forces and long-range repulsive interactions[3]. There are still several open questions regarding to the emergence of striped phases in confined three-dimensional systems. In this work, an approach to characterize the equilibrium configuration of particles subject to an interaction core-corona confined to a 3D cylinder with periodic boundary conditions at both ends is presented.

1.1 Motivation

In recent years, self assembly has been of special interest to the development of microscopic materials due to the formation of intricate and specific structures depending on the thermodynamic variables of the synthesis process[4, 5, 6]. There exist many theoretical frameworks to approximately model and predict phase transitions and equilibrium configurations of complicated systems[7, 8, 9, 10].



Figure 1.1: Some tantalizing natural patterns

1.2 Problem Formulation

To find and characterize the equilibrium configurations of the system.

1.3 Objectives

The general objective of this work is to construct a phase diagram for the system of core-corona particle colloids.

1.3.1 Specific Objectives

The specific objectives of this project are as follows:

- To find the configurations of equilibrium of the system
- Assign an order parameter

- Observe the effect of varying the physical parameters
- Study the results

1.4 Thesis Structure

The thesis is organized as follows:

- Chapter 2 is a survey of the relevant literature
- Chapter 3 is a report of the methods used
- Chapter 4 shows the results and discussion
- Chapter 5 presents the conclusions

Literature Survey

Provide various analysis and research made in the field of your proposal and the results already published or existing products.

2.1 Background

2.2 Colloids

A colloid is a mixture of two species, one called the continuous phase and the dispersed phase. In a colloid the dispersed phase forms aggregates of small size, between 1 and 1000 nm, in the continuous phase. The two phases can be in any state of matter (except when both are gases) and the different combinations receive different names:

		Dispersed phase		
		Solid	Liquid	Gas
Continuous Phase	Solid	Solid sol	Gel	Solid Foam
	Liquid	Sol	Emulsion	Foam
	Gas	Solid aerosol	Liquid aerosol	Not possible

2.3 Block copolymers

A block copolymer is a polymer made out of two different types of monomers.

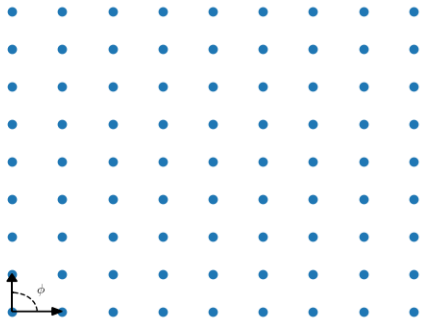
2.4 Two-dimensional Bravais Lattices

In crystallography, a lattice is the infinite set of points in space spanned by the linear combination of basis vectors with integer coefficients i.e. points \vec{p} of the form

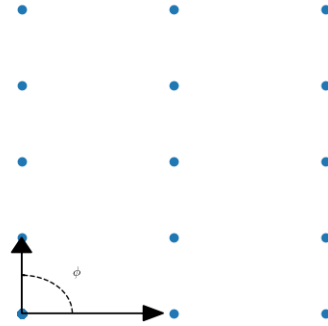
$$\vec{p} = m\vec{b}_1 + n\vec{b}_2 \quad \forall m, n \in \mathbb{N}$$

The grid defined by these vectors has to be invariant for translations by integer multiples of the basis vectors and by rotation about one of the points of the lattice, due to rotational symmetry arguments only five lattices exist in the Euclidean plane[11].

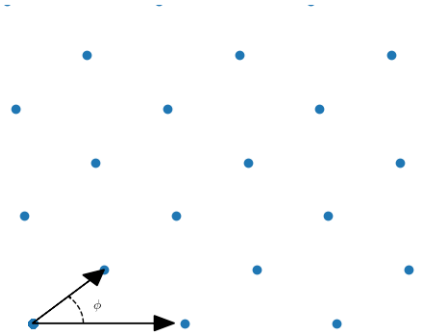
The following four kinds of lattices serve to illustrate the concept.



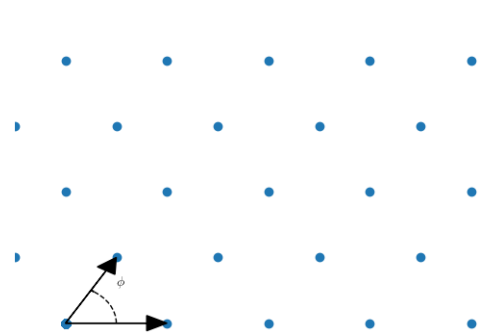
(a) square lattice, $|\vec{b}_1| = |\vec{b}_2|$ $\phi = 90^\circ$



(b) rectangular lattice, $|\vec{b}_1| \neq |\vec{b}_2|$ $\phi = 90^\circ$



(c) oblique lattice, $|\vec{b}_1| \neq |\vec{b}_2|$ $\phi \neq 90^\circ$



(d) hexagonal lattice, $|\vec{b}_1| \neq |\vec{b}_2|$ $\phi = 60^\circ$

2.5 Coordination number

In chemistry the coordination number of a species is the number of species it is bonded to. In the case of this work the coordination number is the number of particles that interact with a given particle.

2.6 Sphere packaging

The problem of finding the most efficient way to pack hard spheres (i.e. spheres that can't intersect each other) in three dimensions is an old problem in geometry. Gauss proved that the FCC lattice is the most efficient of the lattice packagings and it was only recently proven in 2014 by László Fejes Tóth that this lattice is the most efficient packaging in three dimensions for spheres of the same size. This problem is of interest in material science since the structural arrangement determines many

properties of the material. There have been several studies about confined spheres, soft and hard, in several geometries[12, 13, 14, 15, 16, 17, 13, 18, 1, 19, 5]. The case of cylindrical confinement in particular is useful to model several important systems in material science[4, 5, 20, 21, 6, 22, 16, 23, 24, 25, 26].

2.7 Statistical Physics

“Statistical mechanics is a probabilistic approach to equilibrium macroscopic properties of large numbers of degrees of freedom”[7]

This branch of physics serves as the bridge between thermodynamics and classical mechanics in the sense that it describes systems that are governed by the usual classical laws of physics but that have so many degrees of freedom (e.g. particle positions, angular velocity speed) that a precise description of each of them is unfeasible. At its core it deals with the description of systems with a large number of degrees of freedom such as gases, liquids and solids. It allows us to calculate averages of relevant quantities that characterize the system such as temperature, pressure, heat capacity and so on.

2.7.1 Statistical ensembles

An ensemble is a set of states of the system compatible with prescribed physical conditions. There exist three ensembles in statistical physics, the microcanonical, canonical, and grand canonical. In a nutshell, the microcanonical is the basic building block of the other two. The microcanonical ensemble consists of all the states of the system which have the same energy. The canonical ensemble is an ensemble of microcanonical ensembles and the grand canonical is an ensemble of canonical ensembles. Depending on the system itself we can choose the ensemble that better suits the analysis.

2.7.2 Partition function

In statistical mechanics the partition function of a system is the sum of all possible microstates of the system, with a given Hamiltonian. It is useful for our purposes because it allows us to define a probability distribution to find the system at a given state. The partition function for a system is defined as follows:

$$Z = \int_0^{\infty} g(\varepsilon)e^{-\beta\varepsilon}d\varepsilon \quad (2.1)$$

where $g(\varepsilon)$ is the density of states at a given energy.

Monte Carlo Simulations

In the canonical ensemble, the probability of a macroscopic state with energy ε is given by[8]:

$$P(\varepsilon) = \frac{e^{-\beta\varepsilon}}{Z} \quad (2.2)$$

where $\beta = \frac{1}{k_b T}$, and Z is the partition function of the system. It is possible to associate a probability to the transition between two states ε_n and ε_m by computing the energy difference between them[8]. The probability of an arbitray transition between to states is defined to be[27]:

$$P(\varepsilon_n \rightarrow \varepsilon_m) = \begin{cases} 1 & \Delta\varepsilon \leq 0 \\ e^{-\beta\Delta\varepsilon} & \Delta\varepsilon > 0 \end{cases} \quad (2.3)$$

This is known as the Metropolis algorithm.

For the simulation of soft particles in a cylinder, at a fixed temperature, the implementation of this algorithm is as follows:

1. Place the particles inside the cylinder at random positions
2. Select a particle and give it a small displacement
3. Compute the energy difference between the initial state and the state after the displacement
4. Accept or reject the displacement according to (2.3)
5. repeat step 2

2.8 Reduced units

Many constants and quantities in physical systems are many order of magnitude either above or below our common units, in order to reduce the amount of work and memory usage that comes from handling this quantities, we can introduce a new set of units, known as reduced units, to make the computation more efficient. They can be defined as follows[28]:

$$\begin{aligned} \rho^* &= \rho\sigma^3 & \text{density} & & T^* &= k_B T/\varepsilon & \text{temperature} \\ E^* &= E/\varepsilon & \text{energy} & & P^* &= P\sigma^3/\varepsilon & \text{pressure} \\ t^* &= (\varepsilon/m\sigma^2)^{1/2}t & \text{time} & & f^* &= f\sigma/\varepsilon & \text{free energy} \\ \mu^* &= \mu/(4\pi\varepsilon_0\sigma^3\varepsilon)^{1/2} & \text{chemical potential} & & Q^* &= Q/(4\pi\varepsilon_0\sigma^5\varepsilon)^{1/2} & \text{charge} \end{aligned}$$

Methodology

3.1 Model: Core-corona potential

Colloidal particles and copolymer micelles can be modeled by a potential with a hard core of length σ_0 , surrounded by a repulsive soft corona[29, 21, 4]. The soft corona represents a finite energy penalization of particle-particle overlaps, with magnitude ϵ . The associated range is $\lambda \sigma_0$.

$$\phi(r) = \begin{cases} \infty & r \leq \sigma_0 \\ \epsilon & \sigma_0 < r < \lambda\sigma_0 \\ 0 & r \geq \lambda\sigma_0 \end{cases} \quad (3.1)$$

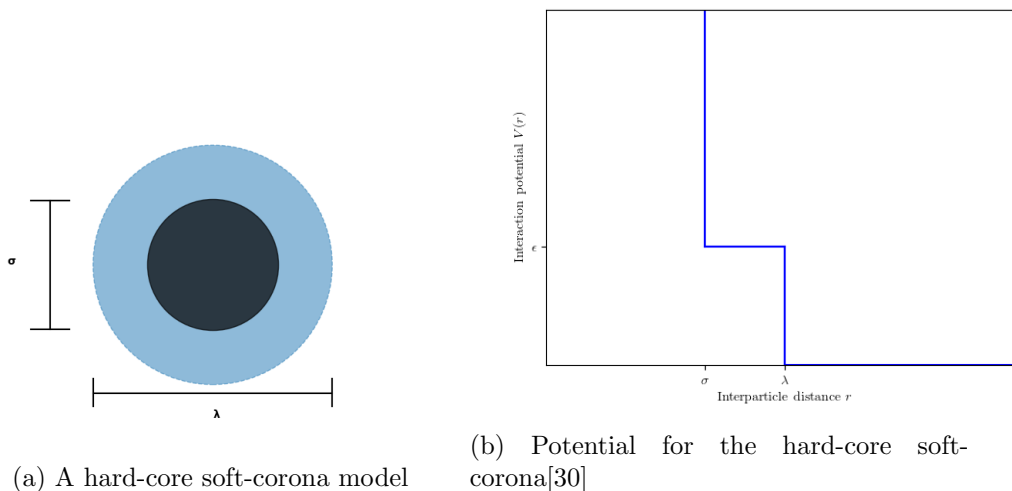


Figure 3.1: Model

For computational convenience, the hard sphere distance of the potential σ is defined to be 1

3.2 Phase-characterization procedure

3.2.1 Hexatic order parameter

The final configurations show the formation of layers within the cylinder. For a better visualization we can isolate the layers formed by the particles in the cylinder. For each particle we define the hexatic order parameter as the module of [31, 32, 17, 15]:

$$\psi_6(\mathbf{r}_m) = \frac{1}{N_b} \sum_{n=1}^{N_b} e^{i6\theta_{mn}} \quad (3.2)$$

where N_b is the number of nearest neighbors. This parameter varies between 0 and 1 and gives a measure of how close the arrangement of neighbouring particles is to a hexagonal lattice.

3.2.2 Mean coordination number

To have another way of classifying the structures the mean coordination number for the whole system was computed. The definition of the coordination number for a given particle in this work is the number of particles that interact with it. The procedure is straightforward:

- Select a particle
- Count all the particles that lie inside of a sphere of radius λ
- Average this for all the particles in the system

3.3 Packaging Factor

The last measure of order for this is the packaging factor of the structure. Again the procedure to compute this quantity for a given layer is straightforward:

1. Isolate and count the number of particles in the layer
2. Measure the radius of the layer
3. Apply the definition of the packaging factor

3.4 Design

The software used to find the equilibrium configurations of the system was written in Fortran by Dr. Abelardo Ramírez Hernández. Small modifications to the source code were required in order to run the amount of simulations presented here.

3.4.1 Monte Carlo simulations specifications

The Monte Carlo simulations are standard NVT, and all had the following parameters all in reduced units:

1. Number of steps : 1×10^8

2. Length of the cylinder: 40
3. Final temperature: $0.1 T^*$

3.5 Implementation

The analysis and characterization of the final configurations obtained from the Fortran program was made with python and automated using Bash scripts. The parameters calculated

The formation of layers in the structure presented the opportunity to use the hexatic order parameter for characterization even when it is defined for two dimensional arrangements. In order to get sensible results, the layers formed were first separated and then projected into a plane through a change of coordinates to avoid any geometrical distortions due to the curvature of the layers.

For the layer formation we also calculated the packaging factor in two dimensions using

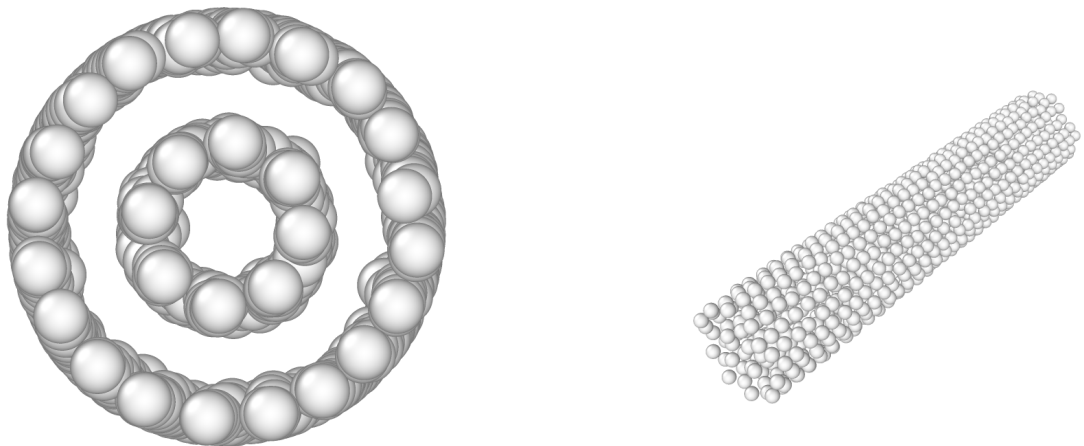
Given that both the calculation of the hexatic order parameter and the mean coordination number required to find the neighbors of a given particle, a tree algorithm[33] was implemented to find the nearest neighbors. This reduces the complexity of neighbor finding from $O(n^2)$ to $O(n \lg(n))$ which saves a considerable amount of time, specially for high density configurations.

Results and Discussion

4.1 Results

In most of the final configurations we can observe the formation of concentric layers along the axis of the cylinder. To analyze and classify the type of structure the hexatic order parameter was computed for each layer according to the procedure discussed in the previous section.

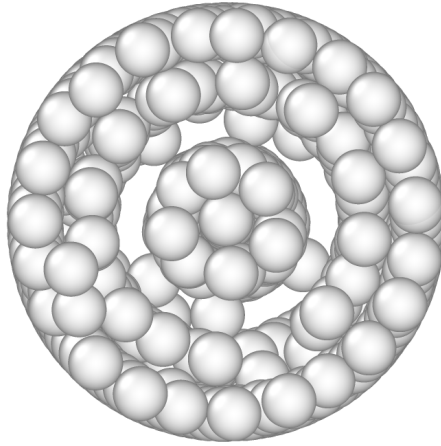
To visualize more easily what was done here are two typical configurations obtained by the simulation[34]:



(a) Top view

(b) Side view

Figure 4.1: Equilibrium configuration for the parameters $\lambda = 2$, $r = 3.5$ $\rho = 0.6$



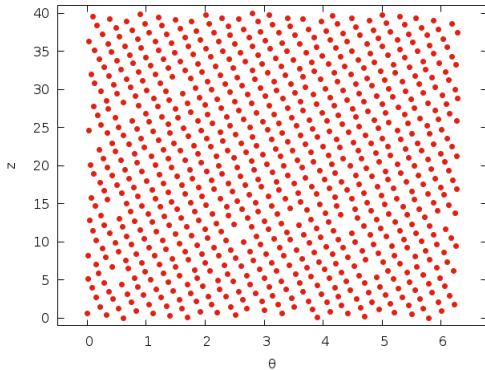
(a) Top view



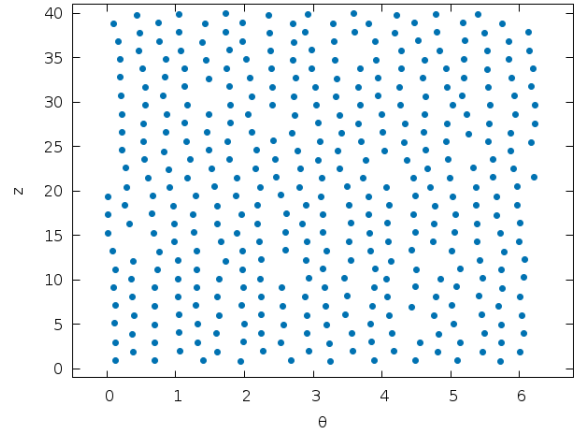
(b) Side view

Figure 4.2: Equilibrium configuration for the parameters $\lambda = 2.5$, $r = 3.5$ $\rho = 1$

The following are the projections of the inner and outer layer for the parameters $\{\lambda = 2.0, \rho = 0.6, r = 4.0\}$ to illustrate the procedure described in the previous section. The hexatic order parameter is calculated in this plane.



(a) Biggest layer



(b) Second biggest layer

Figure 4.3: Projection of the two biggest layers for the parameters $\lambda = 2.0$, $r = 4.0$ $\rho = 0.6$

And now for something completely different. The following graphs represent the value of the *order parameters* discussed in the previous section. Each of them is for a fixed cylinder radius, as discussed before the two larger layers were separated and the order parameters were calculated for each one.

The following diagrams correspond to the second largest layer the missing dots correspond to configurations where only one layer was formed

4.1.1 Hexatic order parameter

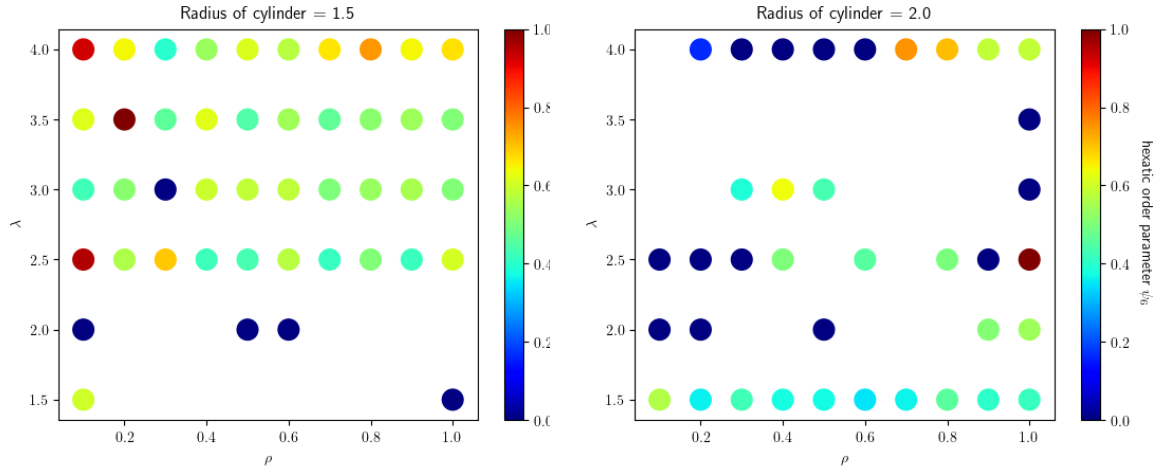


Figure 4.4: hexatic order parameter of the second biggest layer

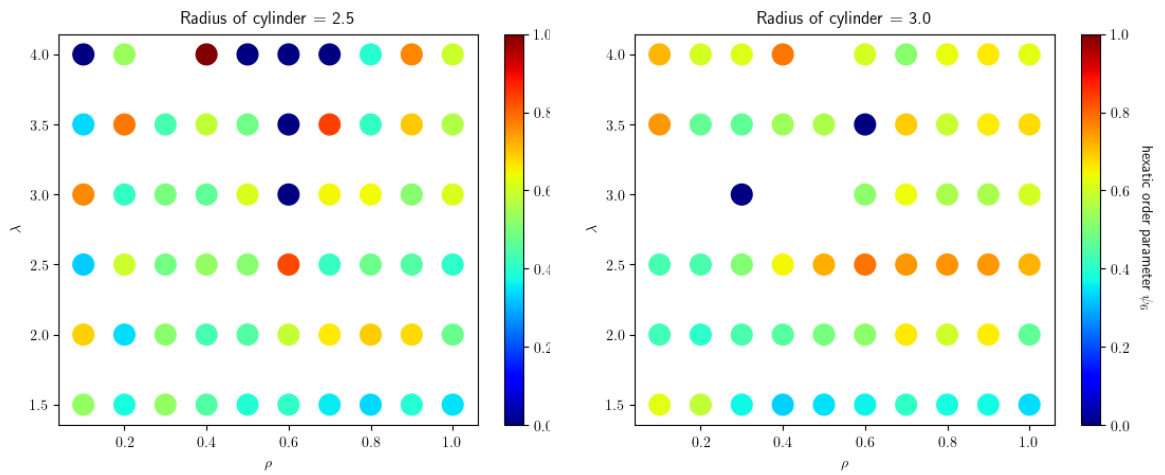


Figure 4.5: hexatic order parameter of the second biggest layer

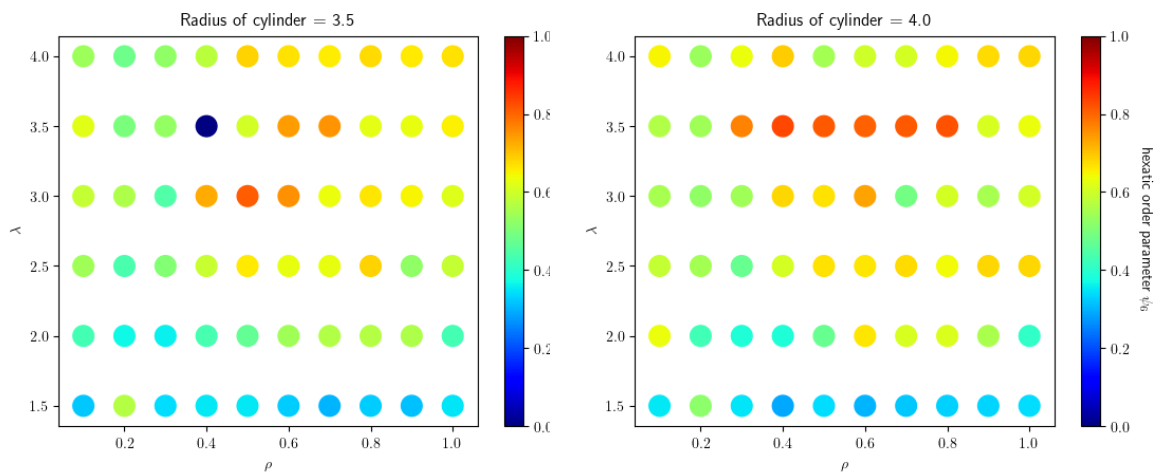


Figure 4.6: hexatic order parameter of the second biggest layer

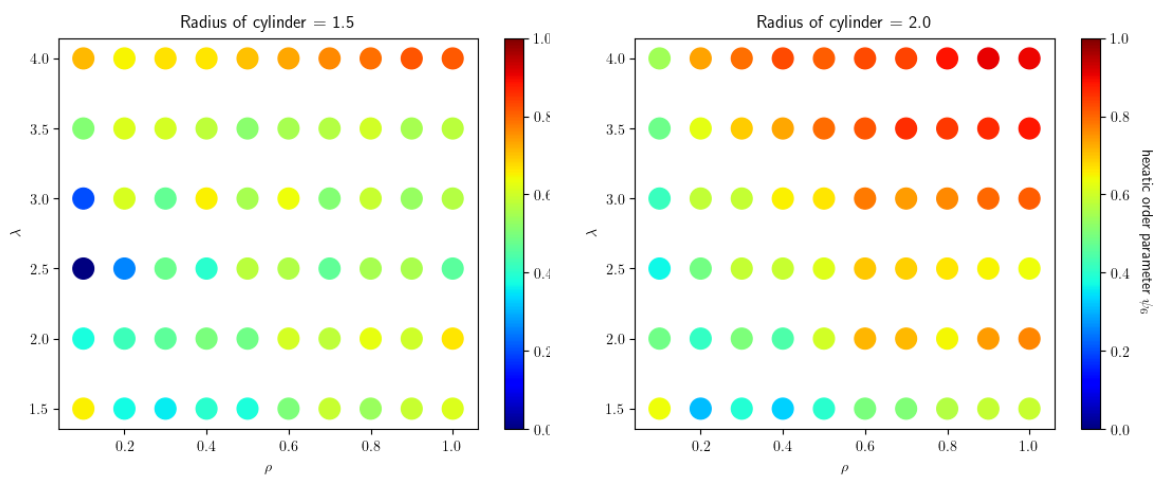


Figure 4.7: hexatic order parameter of the biggest layer

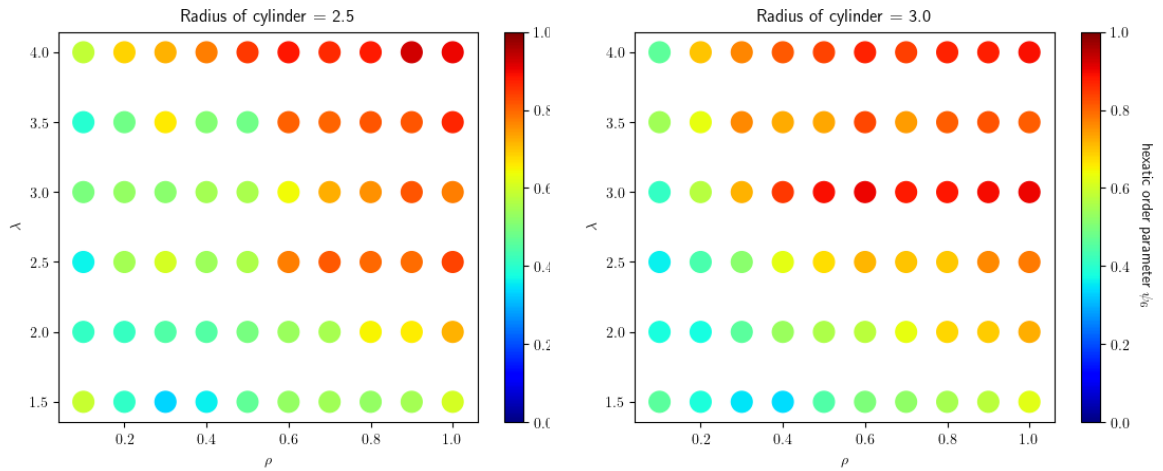


Figure 4.8: hexatic order parameter of the biggest layer

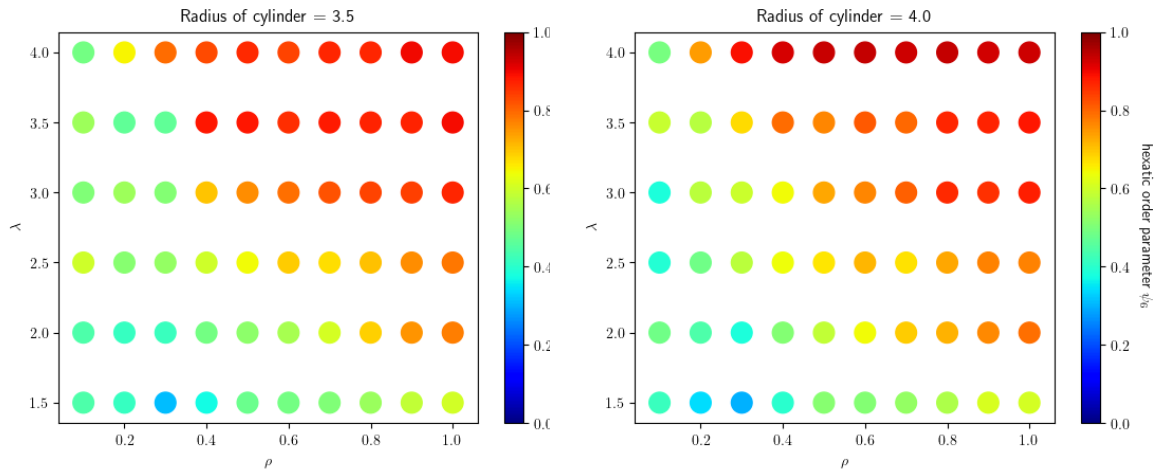


Figure 4.9: hexatic order parameter of the biggest layer

4.1.2 Packaging factor

The quantity presented here is not properly a packaging factor because the layer is defined with a small volume but we use the definition for a two dimensional system. This is why the number presented here is bigger than the most efficient packaging factor in two dimensions ($\frac{\pi\sqrt{3}}{6} \approx 0.9069$)

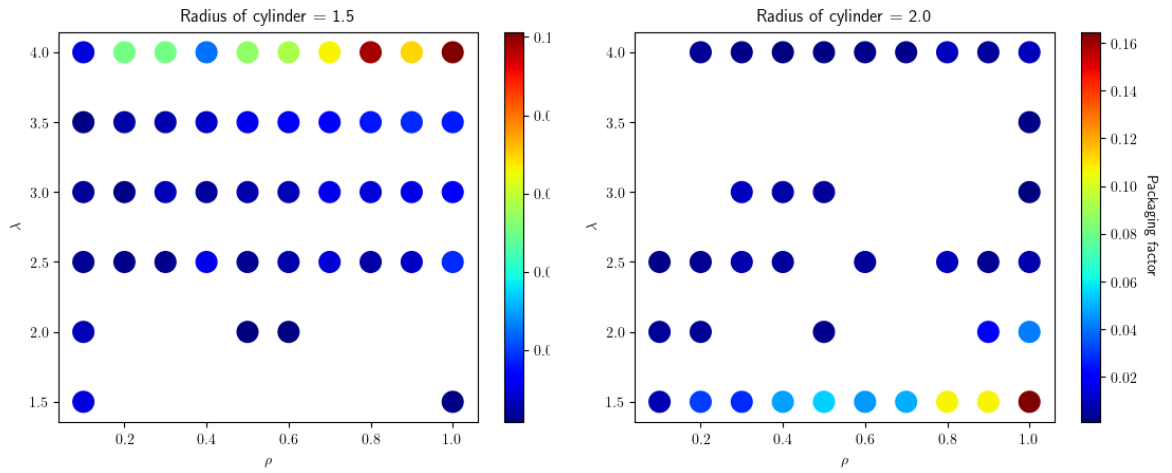


Figure 4.10: packaging factor of the second biggest layer

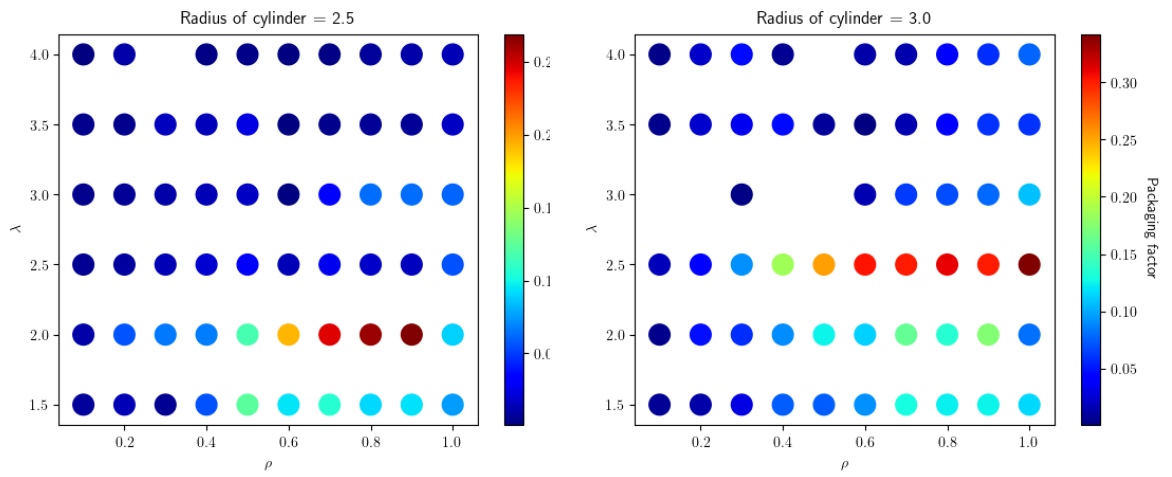


Figure 4.11: packaging factor of the second biggest layer

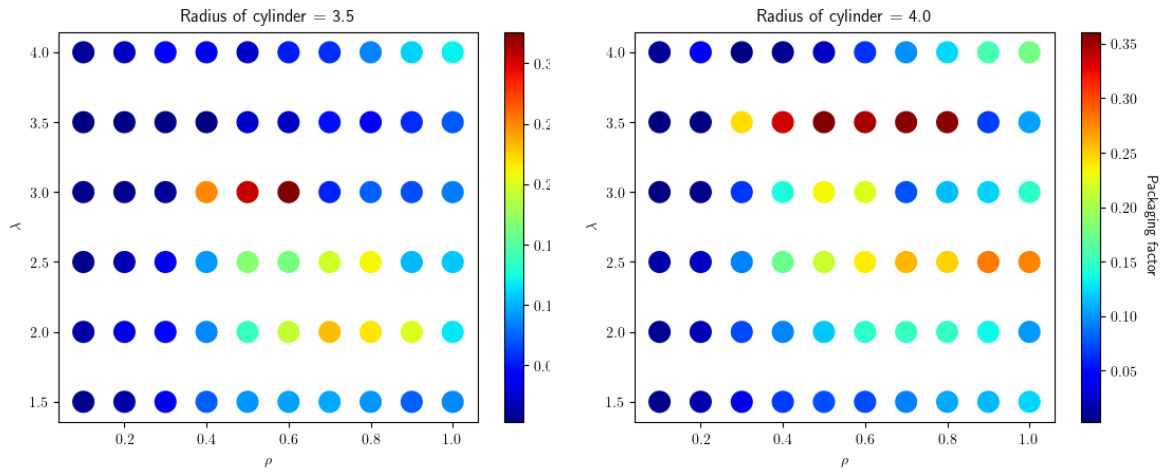


Figure 4.12: packaging factor of the second biggest layer

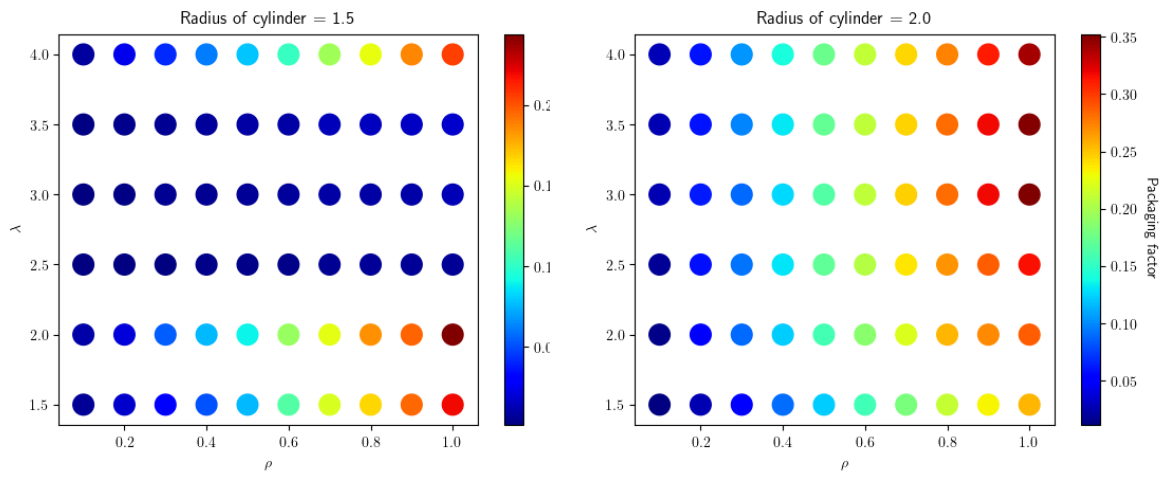


Figure 4.13: packaging factor of the biggest layer

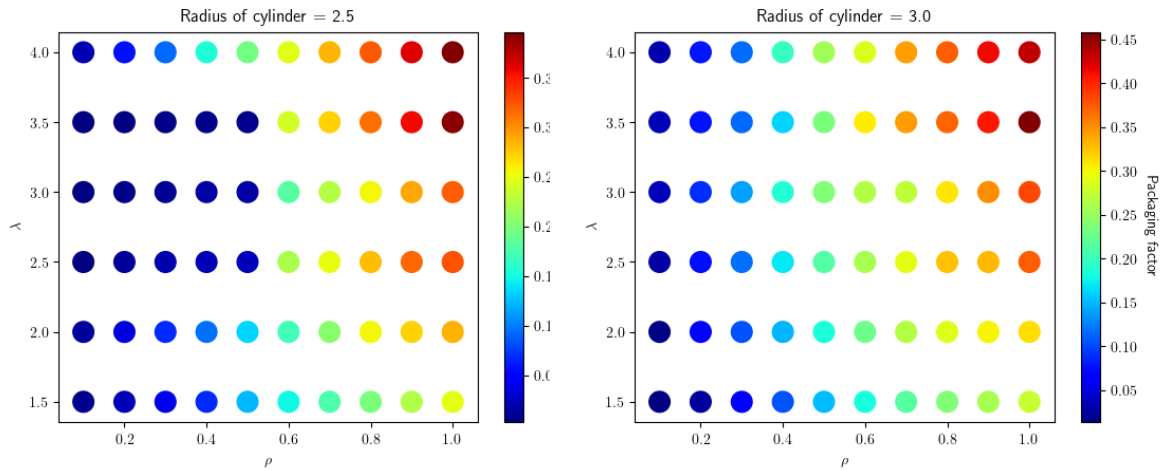


Figure 4.14: packaging factor of the biggest layer

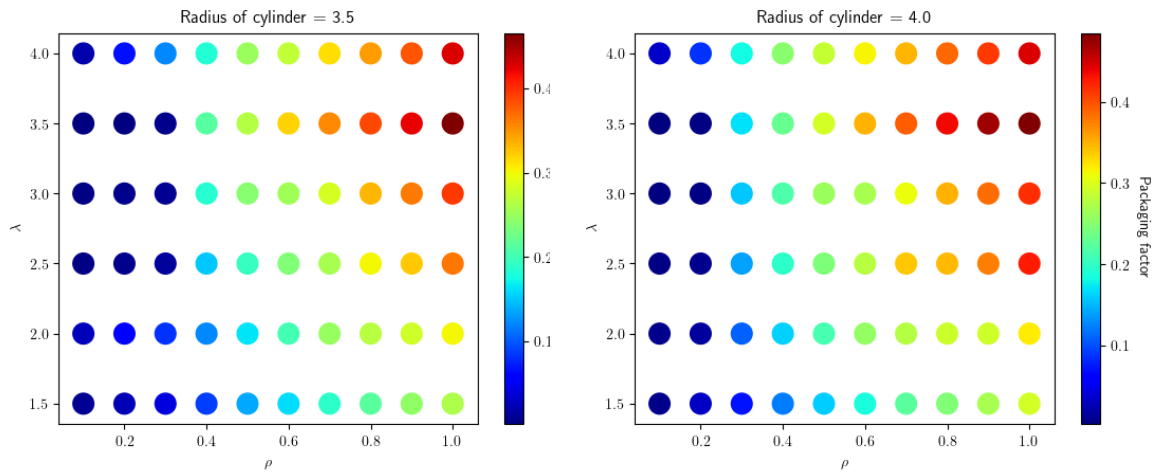


Figure 4.15: packaging factor of the biggest layer

4.1.3 Coordination number

As stated previously, in this work the coordination number for a given particle is the number of other particles that interact with it i.e. the particles at a distance less or equal than λ , this defines a sphere of radius λ around the considered particle.

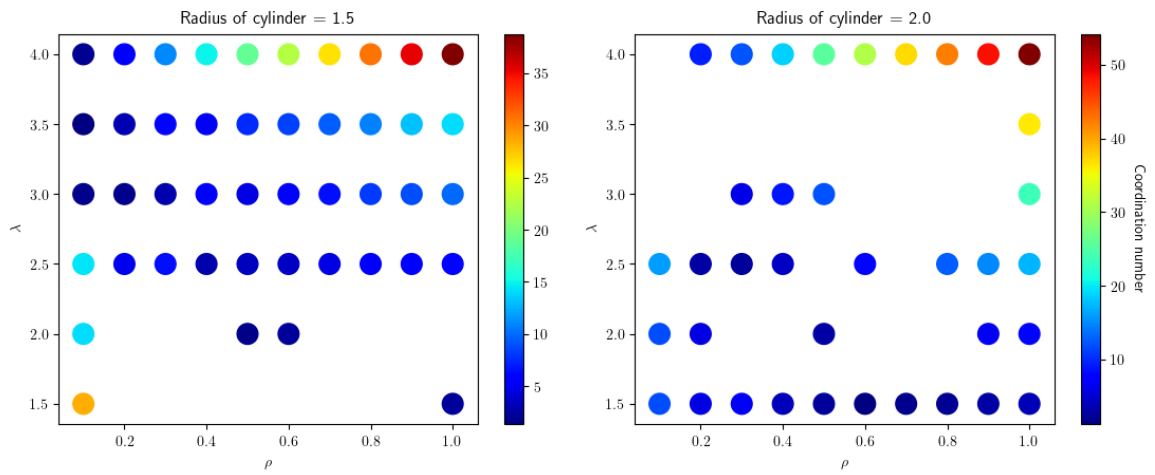


Figure 4.16: average coordination number of the second biggest layer

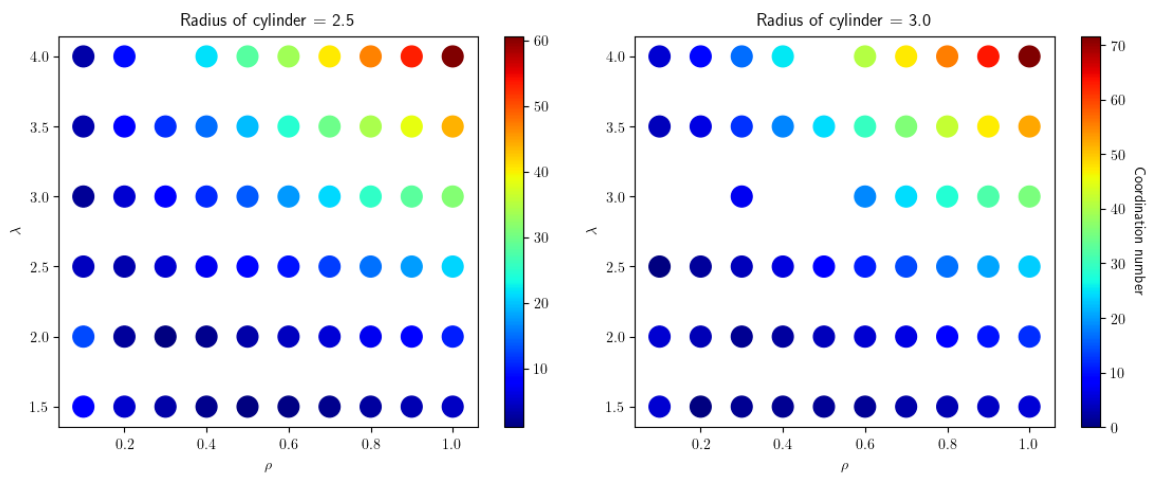


Figure 4.17: average coordination number of the second biggest layer

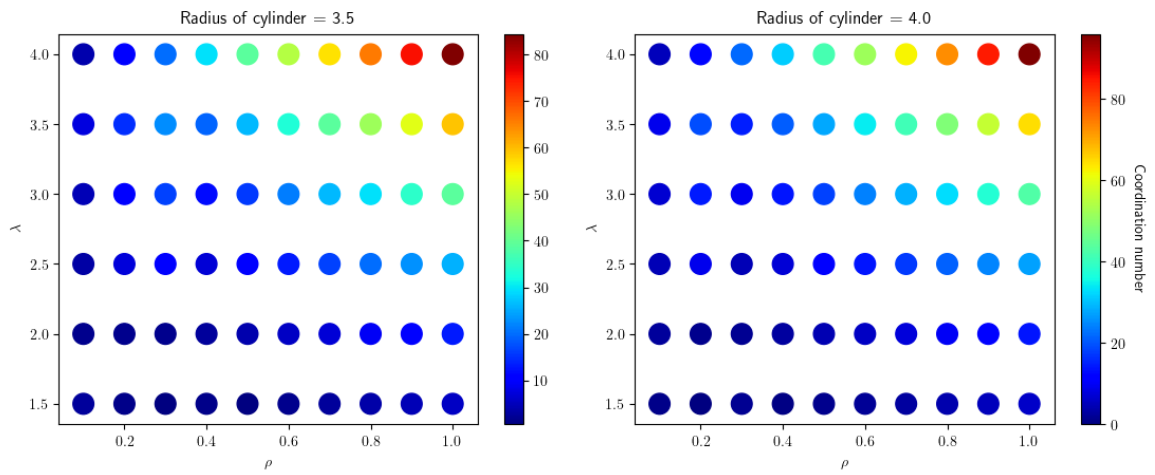


Figure 4.18: average coordination number of the second biggest layer

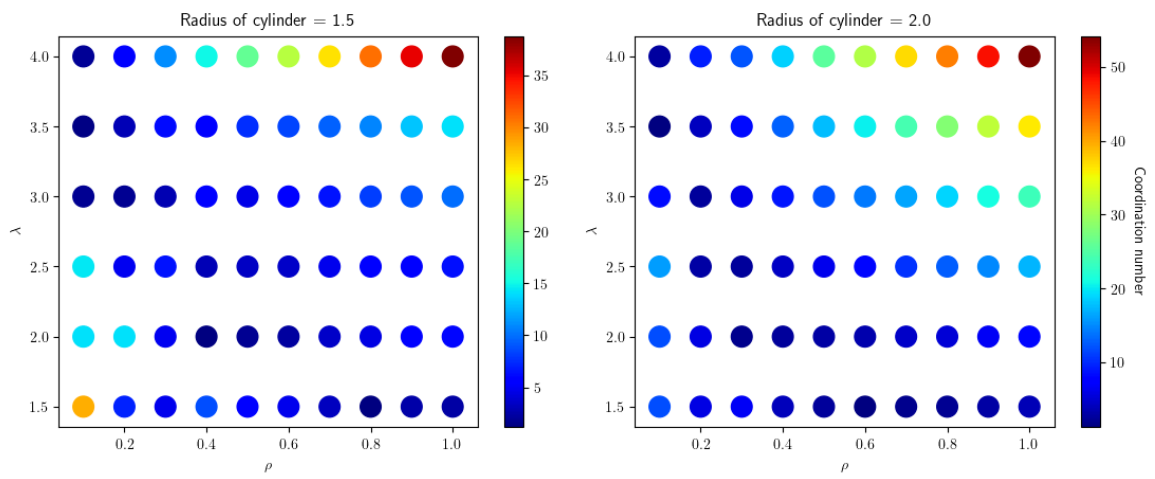


Figure 4.19: average coordination number of the biggest layer

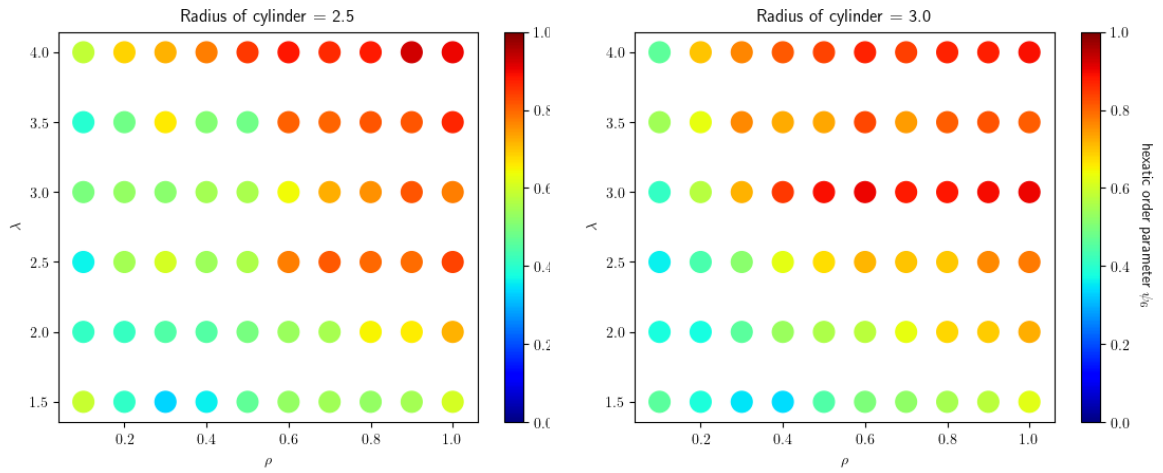


Figure 4.20: average coordination number of the biggest layer

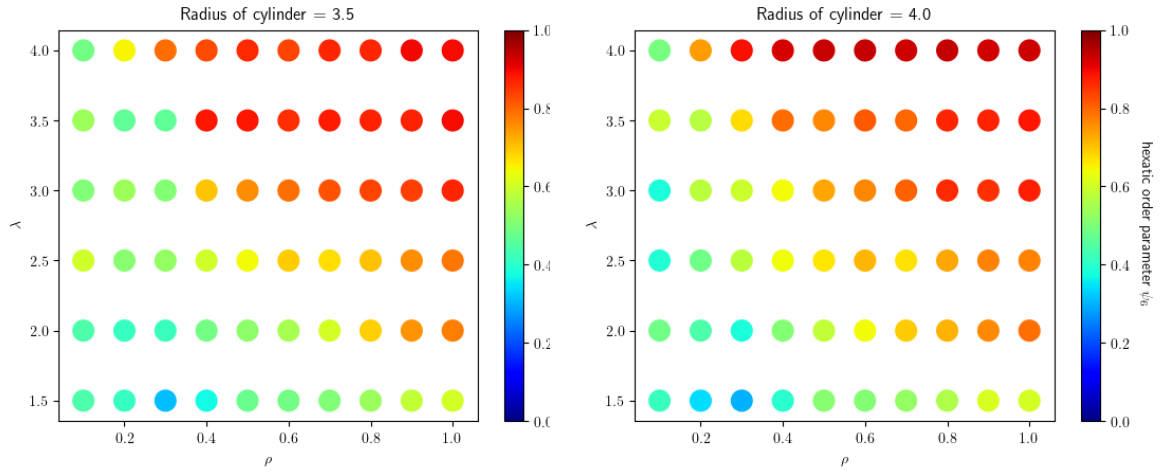


Figure 4.21: average coordination number of the biggest layer

It is worth mentioning that for high values of λ , the system took unexpected configurations that could not be fully characterized with just the methods presented here.

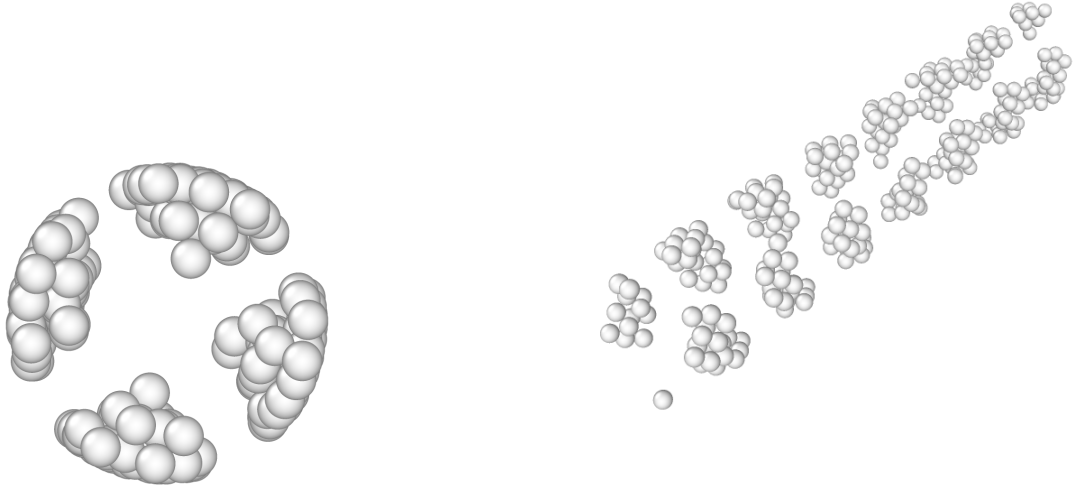


Figure 4.22: An unexpected configuration. $\lambda = 4$ $\rho = 0.2$ $r = 3.5$

4.2 Discussion

With the results obtained we can observe that the length of the soft part of the interaction potential λ is key to the self-assembly of the particles. Since the energy is directly determined by the sum of all the individual coordination numbers the minimum energy configuration of the system requires the minimization of interactions between particles. For a small soft-corona and low densities, there are a wide array of energetically equivalent configurations, the majority of which have no order. As λ increases, the spheres have to arrange themselves in order to avoid touching each other and this gives rise to ordered phases. In some cases like in figure 4.2 we can even observe the formation of crystalline domains in the structure, this is something that was not expected to occur and there is no way to quantify this with only the methods presented in this work.

We can also notice that the numerical density of the system ρ is another key factor to the formation of structured configurations. For systems with a low number of particles we have many equivalent low energy configurations in which the soft part of the spheres isn't touching and thus self-assembly is not favored. As the density grows, the least energy configurations start to show more structure due to the direct relation of the energy to the coordination number.

Although we can have an intuitive reason for the self-assembly of the spheres, the kind of order that will emerge from a certain combination of physical parameters is not at all obvious, at least at the time of writing this, and is evidence that complexity can and will arise even for toy models like the one presented here. The model has many implicit simplifications, and one of the most interesting is the role the continuous phase of colloid has. In this work, the interaction is neglected.

4.3 Significance/Impact

The significance of this work lies in the presentation of the configurations encountered and the systematic classification in the form of a phase diagram that can serve as a rough guide to experimentally construct materials with a desired structure.

4.4 Future Work

Refine the methods presented here in order to deliver a more precise description of the ordering.

Calculate physical properties of the configurations for different materials and compare them with can be found in the scientific literature.

The results obtained so far are a motivation to develop a theoretical framework to explain and predict what kind of configurations are possible and where they can be found. Right now all the work has been done computationally and by running an extensive search on the space physical parameters so it would be helpful to have a rough guide for choosing the combination of parameters. On the other hand it would be interesting to conduct the experiments for some of the unexpected configurations and compare the model to a real system.

Conclusion

The main objective of this work was to build a phase diagram for the system considered. The diagrams constructed with the different order parameters introduced serve this purpose. An ordering of the system can be seen for certain combination of parameters. This ordering was successfully measured using three quantities, the hexatic order parameter, the packaging factor and the mean coordination number. These results were successfully presented as a phase diagram for the density ρ and the interaction length λ . As discussed in the previous section, we can see that both play an important part in the emergence of order in the system. The effect of increasing ρ is associated with the formation of closed packaging, measured in this work by the hexatic order parameter, while the effect of increasing just λ results in the formation of structures with different kinds of ordering such as the one shown in figure 4.22.

Bibliography

- [1] A. Mughal, H. K. Chan, D. Weaire, and S. Hutzler, “Dense packings of spheres in cylinders: Simulations,” *Physical Review E - Statistical, Nonlinear, and Soft Matter Physics*, vol. 85, no. 5, 2012.
- [2] S. Sacanna, D. J. Pine, and G.-R. Yi, “Engineering shape: the novel geometries of colloidal self-assembly,” *Soft Matter*, vol. 9, no. 34, p. 8096, 2013.
- [3] G. Malescio and G. Pellicane, “Stripe phases from isotropic repulsive interactions,” *Nature Materials*, vol. 2, no. 2, pp. 97–100, 2003.
- [4] R. Liang, J. Xu, R. Deng, K. Wang, S. Liu, J. Li, and J. Zhu, “Assembly of polymer-tethered gold nanoparticles under cylindrical confinement,” *ACS Macro Letters*, vol. 3, no. 5, pp. 486–490, 2014.
- [5] P. Dobriyal, H. Xiang, M. Kazuyuki, J.-T. Chen, H. Jinnai, and T. P. Russell, “Cylindrically confined diblock copolymers,” *Macromolecules*, vol. 42, no. 22, pp. 9082–9088, 2009.
- [6] J. H. Moon, S. Kim, G.-R. Yi, Y.-H. Lee, and S.-M. Yang, “Fabrication of ordered macroporous cylinders by colloidal templating in microcapillaries,” *Langmuir*, vol. 20, no. 5, pp. 2033–2035, 2004.
- [7] M. Kardar, *Statistical physics of particles*. Cambridge University Press, 2007.
- [8] D. Landau and K. Binder, *A Guide to Monte Carlo Simulations in Statistical Physics*. 2015.
- [9] C. G. Gray, K. E. Gubbins, and C. G. Joslin, *Theory of Molecular Fluids: Volume 2: Applications*, vol. 10. Oxford University Press, 2011.
- [10] P. M. Chaikin, T. C. Lubensky, and T. A. Witten, *Principles of condensed matter physics*, vol. 1. Cambridge university press Cambridge, 1995.
- [11] C. Kittel, P. McEuen, and P. McEuen, *Introduction to solid state physics*, vol. 8. Wiley New York, 1976.
- [12] K. Koga and H. Tanaka, “Close-packed structures and phase diagram of soft spheres in cylindrical pores,” *Journal of Chemical Physics*, vol. 124, no. 13, pp. 13–17, 2006.
- [13] M. Schmidt and H. Löwen, “Phase diagram of hard spheres confined between two parallel plates,” *Physical Review E*, vol. 55, no. 6, p. 7228, 1997.

- [14] R. O. Erickson, “Tubular packing of spheres in biological fine structure,” *Science*, vol. 181, no. 4101, pp. 705–716, 1973.
- [15] F. Durán-Olivencia and M. Gordillo, “Ordering of hard spheres inside hard cylindrical pores,” *Physical Review E*, vol. 79, no. 6, p. 061111, 2009.
- [16] S. Sanwaria, A. Horechyy, D. Wolf, C.-Y. Chu, H.-L. Chen, P. Formanek, M. Stamm, R. Srivastava, and B. Nandan, “Helical packing of nanoparticles confined in cylindrical domains of a self-assembled block copolymer structure,” *Angewandte Chemie International Edition*, vol. 53, no. 34, pp. 9090–9093, 2014.
- [17] M. A. Lohr, A. M. Alsayed, B. G. Chen, Z. Zhang, R. D. Kamien, and A. G. Yodh, “Helical packings and phase transformations of soft spheres in cylinders,” *Physical Review E - Statistical, Nonlinear, and Soft Matter Physics*, vol. 81, no. 4, pp. 1–9, 2010.
- [18] A. Mughal, H. K. Chan, and D. Weaire, “Phyllotactic description of hard sphere packing in cylindrical channels,” *Physical review letters*, vol. 106, no. 11, p. 115704, 2011.
- [19] M. Z. Yamchi and R. K. Bowles, “Helical defect packings in a quasi-one-dimensional system of cylindrically confined hard spheres,” *Physical review letters*, vol. 115, no. 2, p. 025702, 2015.
- [20] O. Gülseren, F. Ercolessi, and E. Tosatti, “Noncrystalline structures of ultrathin unsupported nanowires,” *Physical Review Letters*, vol. 80, no. 17, p. 3775, 1998.
- [21] L. Zhou, Y. Tan, J. Wang, W. Xu, Y. Yuan, W. Cai, S. Zhu, and J. Zhu, “3d self-assembly of aluminium nanoparticles for plasmon-enhanced solar desalination,” *Nature Photonics*, vol. 10, no. 6, p. 393, 2016.
- [22] Y. Kondo and K. Takayanagi, “Synthesis and characterization of helical multi-shell gold nanowires,” *Science*, vol. 289, no. 5479, pp. 606–608, 2000.
- [23] D. Chaudhuri and B. M. Mulder, “Spontaneous helicity of a polymer with side loops confined to a cylinder,” *Physical review letters*, vol. 108, no. 26, p. 268305, 2012.
- [24] A. N. Khlobystov, D. A. Britz, A. Ardavan, and G. A. D. Briggs, “Observation of ordered phases of fullerenes in carbon nanotubes,” *Physical review letters*, vol. 92, no. 24, p. 245507, 2004.
- [25] A. Thomas, M. Schierhorn, Y. Wu, and G. Stucky, “Assembly of spherical micelles in 2d physical confinements and their replication into mesoporous silica nanorods,” *Journal of Materials Chemistry*, vol. 17, no. 43, pp. 4558–4562, 2007.
- [26] Y. Kobayashi and N. Arai, “Self-assembly of janus nanoparticles with a hydrophobic hemisphere in nanotubes,” *Soft Matter*, vol. 12, no. 2, pp. 378–385, 2015.
- [27] D. Frenkel and B. Smit, “Understanding molecular simulation: from algorithms to applications,” 2002.
- [28] M. P. Allen and D. J. Tildesley, *Computer simulation of liquids*. Oxford university press, 2017.
- [29] Y. Mai and A. Eisenberg, “Self-assembly of block copolymers,” *Chemical Society Reviews*, vol. 41, no. 18, pp. 5969–5985, 2012.

- [30] C. I. Mendoza and E. Batta, “Self-assembly of binary nanoparticle dispersions: from square arrays and stripe phases to colloidal corrals,” *Europhys. Lett.*, vol. 56004, p. 13, 2009.
- [31] X. Qi, Y. Chen, Y. Jin, and Y.-H. Yang, “Bond-orientational order in melting of colloidal crystals,” *arXiv preprint cond-mat/0603229*, 2006.
- [32] R. E. Guerra, C. P. Kelleher, A. D. Hollingsworth, and P. M. Chaikin, “Freezing on a sphere,” *Nature*, vol. 554, no. 7692, p. 346, 2018.
- [33] D. C. Rapaport and D. C. R. Rapaport, *The art of molecular dynamics simulation*. Cambridge university press, 2004.
- [34] A. Stukowski, “Visualization and analysis of atomistic simulation data with ovito—the open visualization tool,” *Modelling and Simulation in Materials Science and Engineering*, vol. 18, no. 1, p. 015012, 2009.

.1 Codes

A total of 645 lines of python and bash code were written, mainly because of my inexperience as a programmer. The whole set of files including the source-code, the ones used make the figures, the configuration files and bash scripts are in a github repository at:

```
git@github.com:ca-cao/colloids
```

Below is the main python cript used to calculate the several quantities presented in the work.

```
# esto recibe un archivo xyz
# todo en python 3
# python3 config.py *.xyz path
import numpy as np
import sys
from funcs import *
from qtree import *
from octree import *
import matplotlib.pyplot as plt
fname=str(sys.argv[1])
#path=str(sys.argv[2])

# obtener parametros del sistema
lamb,r,rho=getparam(str(sys.argv[1]))
r0=(r+1.5*lamb)

# leer archivo
xyz=np.loadtxt(fname,skiprows=2,usecols=(1,2,3))
npart=len(xyz)

# cambio coord y dist
rtz,dist=cart2cyl(xyz,r0)
plt.plot(dist[:,0],dist[:,1])
pk,npks=pf(dist,2)

# rtz[i,:] -> [x,y,z,r,r*\theta,parametro]
# ordenar con respecto al radio
qsort(rtz,0,len(rtz)-1,3)

# separar las capas
pk,npks=pf(dist,2)
lyrs=lyr(rtz[:,3],pk[:,0],.15)

# parametro de orden para las capas
for i in range(len(pk)):
    hexord(rtz[int(lyrs[i,0]):int(lyrs[i,1]),3:6],.5*lamb)
xyzwrite(rtz,fname[:-4]+"hx"+"xyz",6) # escribe todo en un archivo

# calcular promedio de ncoord
eta=ncoord(xyz,lamb)
nbar=np.dot(eta[:,0],eta[:,1])/float(npart)

for i in range(len(pk)):
    f=open(path+"lyr"+str(i)+'.dat','a')
    avg=np.average(rtz[int(lyrs[i,0]):int(lyrs[i,1]),5])
    p_f=pk[i,1]/(pk[i,0]*2*40)
```